A Smart and Flexible Microgrid With a Low-Cost Scalable Open-Source Controller

LIN ZHU[1], (Senior Member, IEEE),
CHENGWEN ZHANG[1], (Graduate Student Member, IEEE), HE YIN[1], (Member, IEEE),
DINGRUI LI[1], (Student Member, IEEE), YU SU[1], (Graduate Student Member, IEEE),
ISHITA RAY[1], (Member, IEEE), JIAOJIAO DONG[1], (Senior Member, IEEE),
FRED WANG[1,2], (Fellow, IEEE), LEON M. TOLBERT[1], (Fellow, IEEE),
YILU LIU[1,2], (Fellow, IEEE), YIWEI MA[3], (Member, IEEE), BRUCE ROGERS[3], JIM GLASS[4],
LILIAN BRUCE[4], SAMUEL DELAY[5], PETER GREGORY[6], MARIO GARCIA-SANZ[7],
AND MIRJANA MARDEN[7]

[1]Min H. Kao Department of Electrical Engineering and Computer Science, The University of Tennessee, Knoxville, TN 37996, USA
[2]Oak Ridge National Laboratory, Oak Ridge, TN 37830, USA
[3]Electric Power Research Institute, Knoxville, TN 37932, USA
[4]Electric Power Board, Chattanooga, TN 37402, USA
[5]Tennessee Valley Authority, Chattanooga, TN 37402, USA
[6]Green Energy Corporation, Eugene, OR 97402, USA
[7]Advanced Research Projects Agency-Energy, U.S. Department of Energy, Washington, DC 20585, USA

Corresponding author: He Yin (hyin8@utk.edu)

ABSTRACT In contrast with conventional microgrids (MGs) with fixed boundaries, a smart and flexible MG with dynamic boundary is introduced in this paper. Such a MG can dynamically change its boundary by picking up or shedding load sections of a distribution feeder depending on its available power, leading to more flexible operation, better utilization of renewables, smaller size of energy storage system, higher reliability, and lower cost. To achieve a flexible MG, the main challenges in MG design are addressed, including recloser placement, MG asset sizing considering resilience, system grounding design, and protection system design. Meanwhile, a hierarchical structure is employed to design and implement the MG controller. On top of the functions defined in IEEE 2030.7-2018, a few new functions, e.g., online topology identification and PQ balance, are added, while the planned/unplanned islanding and reconnection functions are enhanced. The controller is implemented on a CompactRIO, a general-purpose hardware platform provided by National Instruments (NI), and tested on a controller hardware-in-the-loop setup based on an OPAL-RT real-time simulator and a reconfigurable power electronic converter-based hardware testbed. The test results have validated the performance of the developed controllers. Such a flexible MG and its controller have been deployed at a municipal utility, and part of the controller's functions have been tested on-site.

INDEX TERMS CompactRIO, dynamic boundary, hardware-in-the-loop, hardware testbed, IEEE 2030.7, IEEE 2030.8, microgrid, microgrid design, OPAL-RT.

I. INTRODUCTION

The microgrid (MG) is an emerging technology that integrates distributed energy resources (DERs) to serve both local and/or main grid needs. A MG can operate in grid-connected mode to exchange power with and provide ancillary services to the main grid. It can also operate autonomously in islanded mode to support local loads if the main grid is not available,

as a result of grid maintenance, outage, or simply to be off grid. MGs can have many benefits, chiefly among them: economic benefits for better energy management; environmental benefits in the case of renewable energy based DERs; and reliability and resilience benefits, especially against extreme weather events such as storms, hurricanes, floods, and heat waves [1].

The U.S. Department of Energy (DOE) has defined a MG as "a group of interconnected loads and DERs within clearly defined electrical boundaries that acts as a single controllable

entity with respect to the grid'' [2]. This definition has generally well summarized most existing MGs, which can be conceptually illustrated by Figure 1. The ''standard MG'', or ''conventional MG'' as will be termed in this paper, is represented in the light green zone. It contains DERs (photovoltaic panel (PV), battery energy storage system (BESS), and backup generator), loads, and a Point of Common Coupling (PCC). Note that although the DOE definition does not specify it, the conventional MG usually only has one boundary switch or interface point, i.e., S01 in the case of the MG in Figure 1.
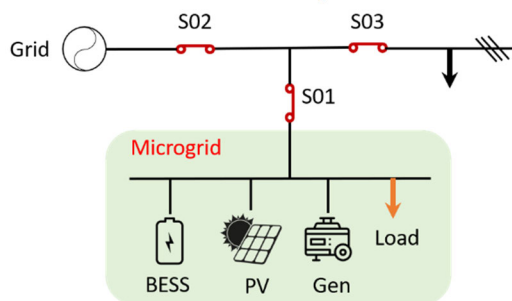

FIGURE 1. Conventional MG with single grid interface.

The conventional MG is a natural configuration for many types of MGs, including campus MGs, military base MGs, commercial MGs, and industrial MGs, where there are clear physical as well as electrical boundaries with a limited number of DERs and relatively small geographical area. The conventional MG is also simple to control with a single PCC and defined DERs and loads.

On the other hand, the conventional MG has limitations. With its single interface point to the grid, the MG may not fully utilize its available generation assets. This is especially true for a community-based MG. To overcome the shortcomings of conventional MGs, the authors have proposed a flexible MG concept with dynamic boundary. The basic concept is illustrated in Figure 2, which has the same system, but its operation is different from that in Figure 1. First, it can have multiple interface points with the distribution grid, G-05 and G-14 in the example given, which allows the MG to reconnect to any available one that is energized. Another important feature is the dynamic boundary. Unlike conventional MGs with a clearly defined fixed boundary, the flexible MG can expand or shrink its boundary by picking up or shedding these load sections according to its available DERs [3]–[5].

In this way, more loads can be served during grid outages to further improve reliability and resilience. Moreover, less energy storage capacity is required since the available power from all the DERs can be utilized by expanding the MG boundary in the islanded mode [6]. For example, in Figure 2(b), Load-10 and Load-11 are not served due to insufficient resources in the islanded MG. However,

they can be served when sufficient resources are available (Figure 2(d)).

Modern utilities are deploying smart switches to divide a feeder into multiple load sections for better fault isolation and load restoration in distribution networks. These smart switches facilitate the implementation of a flexible MG with minimal additional investment. It is noted that regular reclosers or switches that can be remotely controlled to open and close can be also used to implement this flexible MG.

Although flexible MGs with dynamic boundaries provide several benefits, they pose challenges in MG electric system design, MG controller design, and MG controller testing. The next few subsections provide an overview of the state-of-the-art of the aforementioned aspects.

A. MG ELECTRIC SYSTEM DESIGN
The design of MG is a broad topic covering: (1) the siting and sizing of MG assets, (2) the design of the control and communication system, and (3) the design of the protection strategy [7]. There are several existing software tools for conventional MG design, e.g., Hybrid Optimization of Multiple Energy Resources (HOMER) [8], Distributed Energy Resources Customer Adoption Model (DER-CAM) [9], MG Design Toolkit (MDT) [10], and Energy Surety MG [11]. However, none of them can be directly used to design a flexible MG with dynamic boundary.

HOMER has two toolboxes, HOMER Pro and HOMER Grid. HOMER Pro simulates the operation of a hybrid MG for an entire year, in time-steps from one minute to one hour to determine the sizes and combination of MG sources. HOMER Gird is used to optimize behind-the-meter generation to reduce demand charges [8].

DER-CAM is a techno-economic modeling and decision tool, developed to determine the optimal combination of DER generation and storage to minimize energy costs and/or emissions [9]. However, DER-CAM is incapable of designing reclosers to meet reliability requirements.

MDT is another planning tool for MG design. The key capabilities of MDT include the sizing of MGs, cost-benefit analysis, and a simulation tool for performance and reliability analyses [10]. This toolkit provides a broad list of options in the preliminary MG design stage, and thus can reduce the search space. However, the assessment process is heuristic and based on a set of decision rules, and a direct link between reliability indices and MG design is not established.

The Energy Surety MG software includes a design methodology with energy reliability and resiliency as top design priorities [11]. The method uses Monte-Carlo simulations to assess the reliability under equipment failures and attacks and has been applied in the design process of military base MGs. This methodology is primarily developed for critical targets/loads.

B. MG CONTROLLER DESIGN
The main functions of conventional MG controllers are summarized in IEEE 2030.7, which includes (1) device level
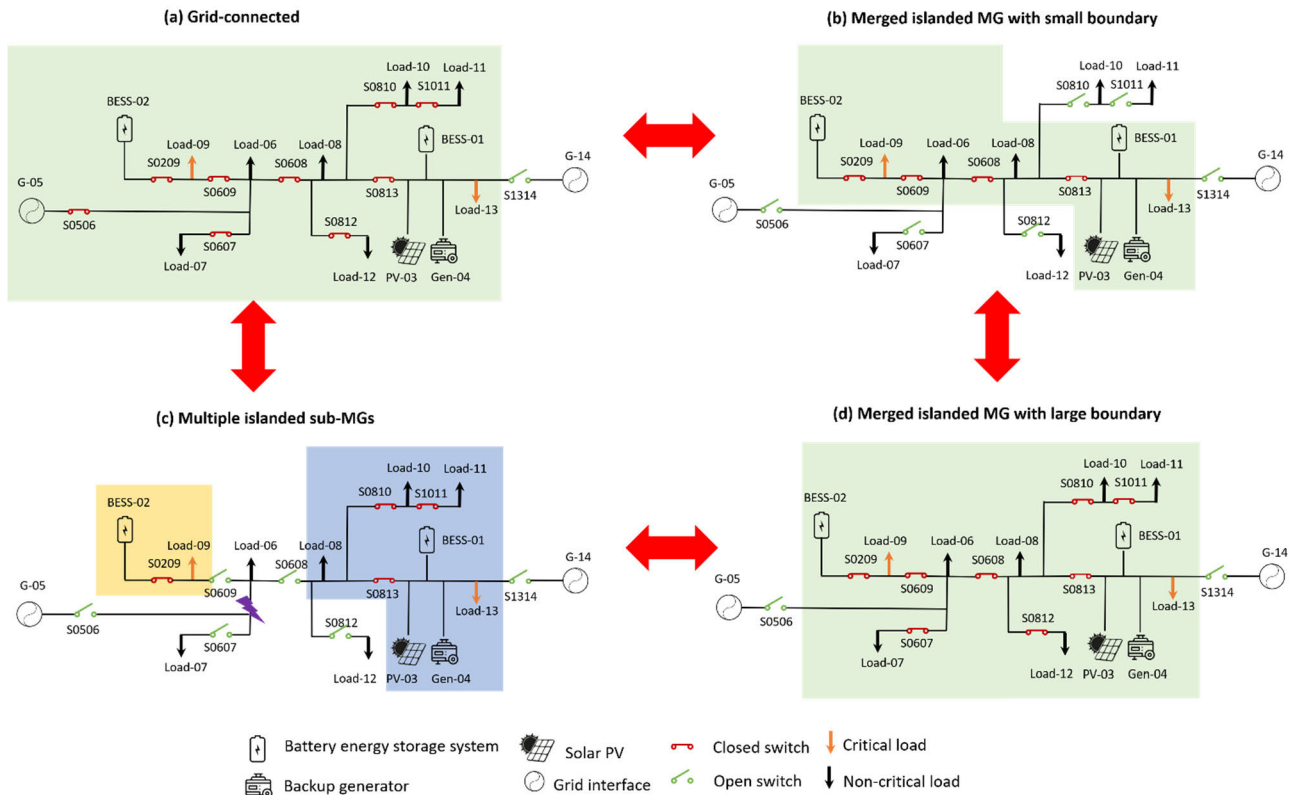
FIGURE 2. Concept of flexible MG with dynamic boundary.

control functions, (2) local area control functions, (3) MG supervisory control functions, and (4) grid interface control functions [12]. There are many commercial MG controllers available in the market that basically follow IEEE 2030.7, e.g., Schweitzer Engineering Laboratories [13], ABB [13], Siemens [14], GE [15], Eaton [16], and Spirae [17]. These controllers have similar functions, e.g., renewable energy source and load forecasting, energy storage systems integration and controls, demand management, etc. However, they need to be modified to enable flexible MG operation with dynamic boundary.

Moreover, there are a few papers that investigate the control algorithms to enable the operation of MGs with dynamic boundary. Schemes to cluster distribution networks into MGs dynamically were proposed in [3] and [18], with the purposes of fully utilizing available DER generation capacity and forming self-adequate MGs, respectively. With dynamic changes in boundary and constant frequency/voltage regulation with various DG modes, a framework for rapid load restoration in [4] is designed to mitigate the impact of faults. However, intended as restoration or MG-forming plans, these methods require prescreening of various operation conditions or case-specific analyses.

To generalize MG formation solutions, a method in [19] formulated the problem as an optimization process to minimize interruptions to critical loads. In addition, investigations have been conducted to extend the flexibility and

performance of MGs with dynamic boundary capabilities by taking advantage of more operation modes of DERs and secondary control strategies [20]–[22]. While these methods predefine, assist, or plan MG boundary changes for load restoration, the computational effort involved becomes a challenge in their application in real-time and dynamic operations.

C. MG CONTROLLER TESTING
Controller hardware-in-the-loop (C-HIL) testing is a popular way to validate the controller performance before deployment. IEEE 2030.8 has defined scenarios, procedures, and metrics to quantitatively evaluate controller performance [23]. The testing scenarios can be divided into six cases: (1) steady-state grid-connected, (2) steady-state islanded, (3) reconnection, (4) planned islanding, (5) unplanned islanding, and (6) black start. The first two cases focus on functions related to dispatch, while other cases focus on functions related to mode transitions. These testing cases can be used to validate flexible MG controllers after certain modifications. While C-HIL is a commonly used and valid testing platform, its effectiveness depends on models. Some of the important features of the controller are often not carefully modeled, notably the communication network, which is important for the MG controller. Moreover, field testing is important prior to a MG controller's integration into a utility's Distribution Management System (DMS)/supervisory

control and data acquisition (SCADA) and for the coordination with protection and control functions in its distribution grids.

This paper introduces a flexible MG with dynamic boundary, including the MG electric system design, MG controller design and implementation, as well as MG C-HIL testing and field testing. As part of integrating the dynamic boundary concept into physical MG controller solutions, specific design problems that were encountered are also addressed in this paper. Moreover, a real-time MG controller is developed, featuring dynamic boundary, flexible grid interface, adaptability to arbitrary topologies, and low-cost deployment [24]–[27]. The controller has been thoroughly tested on an OPAL-RT-based hardware-in-the-loop (HIL) platform and a reconfigurable converter-based hardware testbed (HTB) [28], [29]. Also, some of the controller functions have been tested on a realistic MG owned by a municipal utility.

The rest of the paper is organized as follows. Section II presents the detailed description of the flexible MG with dynamic boundary. The main design challenges of the MG are addressed in Section III. Section IV presents the design and implementation of MG controllers. The C-HIL test results are given in Section V. A realistic flexible MG deployed at a municipal utility and the representative field test results are introduced in Section VI. Finally, Section VII concludes this paper.

II. FLEXIBLE MG WITH DYNAMIC BOUNDARY

Different from a conventional MG "*with clearly defined electrical boundaries that acts as a single controllable entity with respect to the grid,*" the flexible MG introduced in this paper can dynamically change its boundary by picking up or shedding load sections based on the available sources inside the MG when operating in the islanded mode. Meanwhile, due to the dynamic boundary feature, the flexible MG can be connected to any of the adjacent feeders with a dynamic PCC. Moreover, if such a MG has multiple generation or energy storage sources at different locations, the islanded MG can be further split into multiple sub-MGs when necessary (e.g., a permanent fault inside the MG). Also, these sub-MGs can be merged to operate as one MG.

Figure 2 shows an example of such a flexible MG with dynamic boundary for illustration. It has two battery energy storage systems (BESS-01 and BESS-02), one solar PV installation (PV-03), and one backup generator (Gen-04). G-05 and G-14 are the grid interfaces. Load-09 and Load-13 are critical loads, while other loads are non-critical loads. This MG can be separated into two sub-MGs. One is sub-MG #1 with critical Load-13 served by sources BESS-01, PV-03, and Gen-04. The other is sub-MG #2 with critical Load-09 served by source BESS-02 (Figure 2(c)). The main features of the proposed flexible MG are summarized in the following paragraphs. TABLE 1 lists the major differences between the flexible MG introduced in this paper and conventional MG.

A. MULTIPLE GRID INTERFACES

The MG can be connected to the main grid through grid interface G-05 or G-14, using the switch S0506 or the switch S1314 as the PCC, as shown in Figure 2(a).

B. DYNAMIC BOUNDARY

When the MG is operating in islanded mode with low power generation available, it can serve only a few load sections, e.g., Load-09, Load-06, Load-08, and Load-13, as shown in Figure 2(b). On the contrary, with more power generation available, it can expand its boundary by picking up more load sections, e.g., Load-07, Load-10, Load-11, and Load-12, as shown in Figure 2(d).

C. MULTIPLE SUB-MGs

When a fault occurs inside the MG, it can split into two sub-MGs, as shown in Figure 2(c). The two sub-MGs can operate independently, and they can be merged back into one islanded MG by closing the switches S0609 and S0608.

D. DYNAMIC PCC

While the multiple grid interfaces allow the MG to reconnect to the main grid through different PCCs, the dynamic boundary feature also enables dynamic PCC. Taking sub-MG #1 with a large boundary (Load-06, Load-08 and Load-13 are served) for instance, the switch S0506 will be the PCC to the main grid when reconnection is needed. By contrast, if sub-MG #1 has the minimum boundary (only Load-13 is served), the main grid can pick up load sections Load-06 and Load-08, and the switch S0813 becomes the PCC.

E. RECONNECTION

Because the system can have multiple sub-MGs, the reconnection could be more flexible than in conventional MGs. The two sub-MGs could be reconnected to the main grid individually, or they could be merged before reconnecting to the main grid.

F. PLANNED/UNPLANNED ISLANDING

Similarly, the multiple sub-MGs allow more flexible islanding operations. The grid-connected MG can become one islanded MG or multiple sub-MGs through planned or unplanned islanding. Also, one merged MG can be split into multiple sub-MGs through planned or unplanned islanding.

Since the flexible MG can expand its boundary in case of extra power, the renewables can be fully utilized to serve more load sections without unnecessary curtailment. Also, the required capacity of BESS can be much smaller than conventional MGs. Although the flexible MG can bring significant benefits, it puts more requirements on design and operation to achieve a MG with dynamic boundary. First, the feeder needs to be divided into different load sections to allow the MG to change its boundary. Second, due to flexible PCC, the design of protection schemes will be more challenging because different protections or settings are needed

TABLE 1. Comparison between conventional MGs and flexible MGs.

	Conventional MG	MG introduced in this paper
Grid interfaces	Single grid interface (typically)	Multiple grid interfaces (Connected to one of multiple possible adjacent feeders)
Boundary	Fixed boundary	Dynamic boundary
Sub-MG	Cannot split into multiple sub-MGs (typically)	Can split into multiple sub-MGs
PCC	One, fixed PCC	Multiple, dynamic PCC
Reconnection	Reconnect islanded MG to the main grid	• Reconnect islanded sub-MGs to the main grid individually • Merge multiple islanded sub-MGs before reconnection
Planned or unplanned islanding	One MG from grid-connected to islanded mode	• Grid-connected to one merged islanded MG • Grid-connected to multiple islanded sub-MGs • One merged MG to multiple islanded sub-MGs

depending on the operating condition of the MG. Third, the MG controller needs to have advanced functions to enable the operation of a MG with dynamic boundary. Finally, since the load sections can be controlled by both DMS/SCADA and the MG controller, the coordination between the two is required.

III. DESIGN OF MG WITH DYNAMIC BOUNDARY
In this section, the specific design problems of the proposed flexible MG with dynamic boundary are addressed, including recloser placement, MG asset sizing considering resilience, grounding system design, and protection system design.

A. RECLOSER PLACEMENT
Feeder segmentation is essential for the flexible MG to dynamically change its boundary. Modern distribution utilities are deploying smart reclosers for fast fault isolation and service restoration. These smart reclosers with built-in telemetry functions, communication, and remote control capabilities can facilitate the implementation of MGs with dynamic boundary. It is noted that regular reclosers and normal switches with remote control can also meet the requirements of dynamic boundary operation.

These reclosers are normally evenly installed along the main trunk line based on the number of customers or connected loads. However, depending on the reliability requirement for the critical load, it may be needed to place an additional recloser close to the critical load to create a small line section that has a minimal failure rate. The calibrated failure rates and repair time (or the estimated values) of the overhead line or underground cable are used to determine the maximum length of the section containing the critical load, based on the expected system average interruption duration index (SAIDI) target. The maximum section length can be obtained by

$$SectionLength_{max} = \frac{TargetSAIDI}{FailureRate \times RepairTime} \quad (1)$$

If the feeder has no reclosers, the MG designer can use the Sensor Placement Optimization Tool (SPOT) to determine the optimal placement of reclosers. The mathematical

formulation used by SPOT can be summarized below:

$$\min_{N_{add}} \; Reliability \; index \quad (2)$$

$$s.t. \; Reliability \; index = f\left(N_{existing}, N_{add}\right) \quad (3)$$

$$0 \le N_{add} \le N_{max} \quad (4)$$

$$N_{add} \in N_{constraint} \quad (5)$$

where $N_{existing}$ is the existing reclosers, N_{add} is the added reclosers, N_{max} is the maximum number of the added recloser, and $N_{constraint}$ represents the physical constraints.

The objective (2) is to minimize the system reliability indices, e.g., SAIDI, by installing N_{add} reclosers. Other user-defined objectives can also be included, such as customer interruption cost. The system reliability index (3) is a function of the recommended reclosers and $N_{existing}$ pre-existing ones. The number of reclosers is limited in (4) by N_{max}. The constraints in (5) include practical constraints, such as the peak load of each section, maximum number of customers of each section, maximum distance between adjacent reclosers, and location restricted to the three-phase main trunk of the feeder, etc. The reliability indices are calculated through a Monte Carlo simulation to determine the optimal number and location of the reclosers. More details about recloser placement for MG with dynamic boundary will be reported in a separate paper.

B. MG ASSETS SIZING CONSIDERING RESILIENCE
During extreme weather, especially in the night when no PV generation is available, the critical load will be mainly supported by the BESS and/or backup generator. The optimal battery and backup generator sizing problem considering the stochastic event occurrence time and duration is investigated. The resilience requirement is quantified by the mean value of the critical customer interruption time in each stochastic islanding time window (ITW). The ITW length is the duration, and the ITW center is the occurrence time. The stochastic ITW constraint can be transformed to a probability-weighted expression to derive an equivalent Mixed Integer Linear Programming model. More details can be found in [30].

While the energy capacity of the BESS is determined using total cost and reliability under extreme events as criteria,

the generation and load mismatch should be considered for the power rating of the BESS. The power capacity can be determined by the maximum positive power mismatch, or a certain statistic percentile of the power mismatch. Since there may be outliers in the power mismatch data, it may be impractical to design the generator capacity based on the maximum power mismatch. Alternatively, a certain percentage (80% - 95%) of the maximum power mismatch can be used. There is a tradeoff between the absolute availability (the ability to support the entire load of the MG during transitions) and cost (higher power rating leads to higher battery system cost).

C. SYSTEM GROUNDING

In a MG, grounding provides a zero-sequence path for the system [31]. In grid-connected mode, the MG grounding is obtained from the main distribution grid. However, in an islanded MG, the grounding source from the main grid is isolated from the MG, and so the islanded MG requires its own separate grounding, which must be designed.

Delta-Yg connected transformer-based grounding scheme is applied as the grounding source for MG islanded operation, which is shown in *Figure 3*. Since the extra grounding transformer may desensitize the grounding relays and decrease the equivalent grounding impedance to increase the ground fault current in the grid-connected mode, a controllable smart switch S_g is utilized to disconnect/connect the grounding transformer in different MG operation modes.
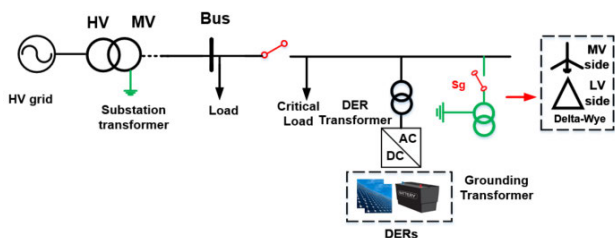

FIGURE 3. Grounding transformer-based grounding scheme.

The sizing of the grounding transformer includes the continuous current rating (power rating), grounding impedance, and thermal rating. The continuous current rating should meet the requirement in (6)

$$I_{continuous} \geq I_{0Lmax} \tag{6}$$

where $I_{continuous}$ is the continuous current rating and I_{0Lmax} is the maximum zero-sequence load current.

The grounding impedance is determined by the single-phase voltage range and temporary overvoltage requirement (TOV). The phase-to-ground voltage is composed of phase to neutral voltage and neutral to ground voltage, which can be written in (7)

$$\vec{V_p} = \vec{V_{pN}} + \vec{V_{Ng}} = \vec{V_{pN}} + \vec{I_0}Z_g \tag{7}$$

where $\vec{V_p}$ is the phase voltage, $\vec{V_{pN}}$ is the phase to neutral voltage, $\vec{V_{Ng}}$ is the neutral to ground voltage, Z_g is the grounding impedance, and $\vec{I_0}$ is the zero-sequence current. For normal operation, since the zero-sequence current is determined by the load and the neutral voltage range is required by the single-phase voltage range, the grounding impedance range Z_{g1} can be estimated by (8),

$$Z_{g1} \leq \frac{5\% \times V_p}{I_{0Lmax}} \tag{8}$$

where V_p is the magnitude of phase voltage value and 5% is the voltage deviation requirement [32]. During a ground fault, the zero-sequence current is determined by the fault current. The phase to neutral voltage is regulated by power inverters or generators, meaning that the phase to neutral voltage is not greater than 1 p.u. (inverter rides through and generator tries to regulate the voltage to be 1 p.u.). Considering the worst case that phase to neutral voltage can be controlled to 1 p.u. based on the TOV requirement, the grounding impedance range is Z_{g2} described in (9):

$$Z_{g2} \leq \frac{38\% \times V_p}{I_{0fmax}} \tag{9}$$

where I_{0fmax} is the maximum zero-sequence fault current, 38% is the TOV requirement [33]. Therefore, the eventual grounding impedance is determined by (10)

$$Z_g \leq min\{Z_{g1}, Z_{g2}\} \tag{10}$$

The reactance to resistance (X/R) ratio of the grounding impedance will impact the asymmetrical peak current during a fault condition. According to IEEE Std C57.32-2015 [34], the asymmetrical peak current rating can be 1.509-2.824 times of transformer thermal current rating with the change of X/R. To limit the asymmetrical peak current to 2 times the transformer thermal current, a transformer with an X/R ratio of 4 should be selected.

The thermal limits of the grounding transformer include thermal current rating and fault toleration time, which are determined by the maximum fault zero-sequence current and fault duration which is determined by the system protection response time. Therefore, the thermal current rating (I_{th}) [34] of the transformer should be larger than the maximum zero-sequence current rating, and the fault toleration time (t_{ft}) should be longer than the system protection response time.

The maximum zero-sequence current of the grounding transformer will also flow through the controllable smart switch S_g, which is the maximum fault zero-sequence current. Meanwhile, since S_g opens in the grid-connected mode to disconnect the grounding transformer, it is required to tolerate the maximum phase to ground voltage in the grid-connected mode. The maximum phase to ground voltage is also determined by the TOV requirement, which requires S_g to tolerate 1.38 p.u. of the phase voltage.

D. PROTECTION SYSTEM DESIGN

A MG with dynamic boundary poses new requirements on MG protection, e.g., selective protection in the islanded mode, and tight integration of MG protection, MG control, and feeder protection/automation. An enhanced protection scheme on top of existing distribution grid protection is recommended [35]. TABLE 2 shows the recommended protections for a grid-connected MG. The existing inverse time overcurrent relays are employed as the grid side relays. When the MG has only inverter-based energy sources, communication-aided overvoltage/undervoltage relays coordinated with inverters' ride-through capability are utilized as the MG side relays. If the MG also has a backup generator, either communication-aided undervoltage/overvoltage relays or inverse time overcurrent relays can be used as the MG side relays.

TABLE 2. Recommended protections for Grid-connected MG.

	Recommended protection	
Main grid side	Inverse time overcurrent relay	
MG side	Inverter-based source only	• Communication-aided undervoltage and overvoltage relay • Direct transfer trip
	Inverter-based source + backup generator	• Communication-aided undervoltage and overvoltage relay; or inverse time overcurrent relay • Direct transfer trip

Similarly, the recommended protections for the islanded MG are given in TABLE 3. Since a fault in the islanded mode will be isolated on the MG side only, the direct transfer trip may not be needed in the islanded mode.

TABLE 3. Recommended protections for Islanded MG.

	Recommended protection
Inverter-based source only	• Communication-aided undervoltage and overvoltage relay
Inverter-based source + backup generator	• Communication-aided undervoltage and overvoltage relay, or • Inverse time overcurrent relay

This recommended protection scheme is a generic protection scheme. The undervoltage/overvoltage relays are independent of inverters' behaviors under fault conditions and system grounding methods. Moreover, the inverse time overcurrent relay can be utilized as the MG side relay only when the MG has a backup generator. The settings of the inverse time overcurrent relay are mainly determined by the fault current contributed by the backup generator. Therefore, the protection design is much simpler.

IV. MG CONTROLLER DEVELOPMENT

The proposed MG control system contains two parts: MG central controller (MGCC) and MG local controllers (MGLCs). While the algorithms and methodology for MGCC and MGLCs are generic, they have been implemented on National Instruments (NI) general purpose hardware platform - CompactRIO, using LabVIEW as the programming language. In the following subsections, the MGCC and MGLCs, and their implementations on CompactRIO will be introduced in detail.

A. MICROGRID CENTRAL CONTROLLER

The architecture of the MGCC consisting of 17 function blocks and their relationship is shown in Figure 4. All function blocks read their initial settings from the model management function, where the initial settings are stored in the internal memory of the controller. The communication function block provides up-to-date information on switches, sources, and SCADA to all other function blocks. With the switches and sources information, the topology identification function generates the current MG topology and shares the topology information with other functions. The selected functions with unique features are introduced below.

1) FINITE STATE MACHINE (FSM)

The FSM determines the MG operation state according to the MG topology. With the multiple source MG feature, the FSM function has multiple states for multiple sub-MGs. Meanwhile, the FSM generates the function block enable/disable flags to trigger and coordinate the functions. The functions usually work independently in parallel when given the enable trigger from the FSM. The advanced functions, such as PQ balance, planned islanding, reconnection, and energy management functions, cooperate with each other to achieve these intricate controls. For instance, the planned islanding function uses the internal signals and information from PQ balance and topology identification functions to generate the source power and switch status control which will be discussed in Section VI.

2) TOPOLOGY IDENTIFICATION

This function is designed to automatically process the real-time MG topology and determine the MG boundary based on smart switch status. It monitors the smart switch statuses through the communication function block and then generates the MG real-time topology matrix using Kruskai's algorithm-based searching method [27]. In the generated topology matrix, the loads and sources sectionalized by smart switches are represented by nodes, and the smart switches are represented by lines.

3) PQ BALANCE

The PQ balance function is designed to balance the active and reactive power within a MG or multiple sub-MGs by automatically changing the MG boundaries and controlling the energy resources (PV, BESS, backup generator). It also initiates the separation and merging of (sub-) MGs.

4) PLANNED/UNPLANNED ISLANDING

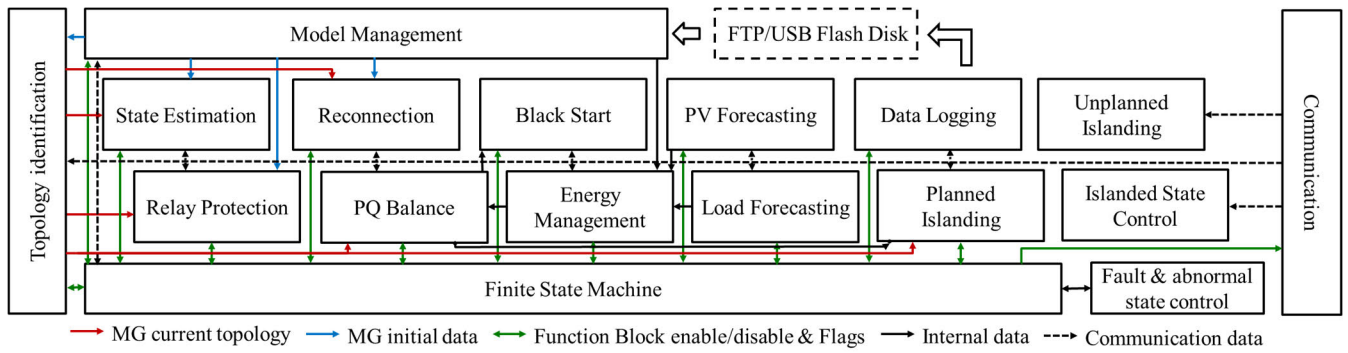The planned and unplanned islanding and reconnection functions are modified to enable islanding from the main grid on

FIGURE 4. Function blocks and their relationships in MGCC.

multiple PCC locations. Also, it allows the controller to split the MG into multiple sub-MGs.

5) RECONNECTION
Similarly, the reconnection function is enhanced to allow the reconnection through multiple PCC locations and the reconnection of multiple sub-MGs. Multiple sub-MGs can either be reconnected to the main grid individually in sequence or be merged into one islanded MG first and then be reconnected to the main grid at once.

B. MICROGRID LOCAL CONTROLLER
The MGLC function blocks and their relationship are shown in Figure 5. Note that, there are multiple MGLCs in the MG control system. Among the seven function blocks, three of them are bridging signals and information for the other four independent functions. Unlike the MGCC, the MGLC functions require less coordination through high-level blocks.
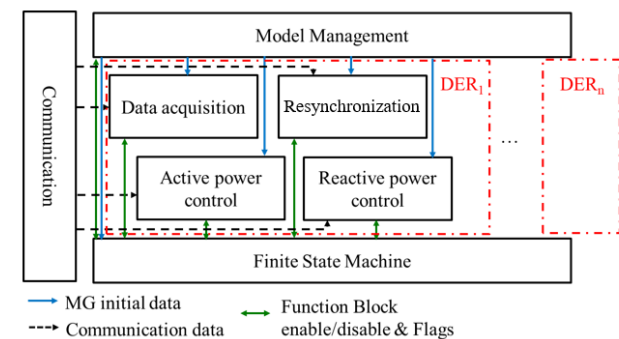

FIGURE 5. Function blocks and their relationships in MGLC.

In addition, because of the multiple source MG feature, one MGLC can be controlling multiple DERs, as shown in Figure 5. Each DER is controlled independently with its dedicated function blocks in the shared MGLC.

V. CONTROLLER HARDWARE-IN-THE-LOOP TEST
To validate the performance of the developed controllers in a C-HIL setup before deployment in the field, this section

introduces two such testing setups, one based on OPAL-RT simulator, and the other is a reconfigurable converter-based HTB. Representative test results on the two platforms are also presented.

A. HIL TEST ON OPAL-RT SIMULATOR
1) OPAL-RT HIL TEST SETUP
The first C-HIL testing setup is based on the OPAL-RT real-time digital simulator. As shown in Figure 6, the circuit model is emulated on OP4510, including MG circuit, DERs, and protections. The control system consists of one MGCC and two MGLCs implemented on CompactRIOs. The communication among the controllers and OP4510 is based on Distributed Network Protocol 3 (DNP3), which is widely used in today's distribution grids. Also, a desktop PC is used to deploy the OPAL-RT model to the OP4510 and display the test results on the human machine interface (HMI).
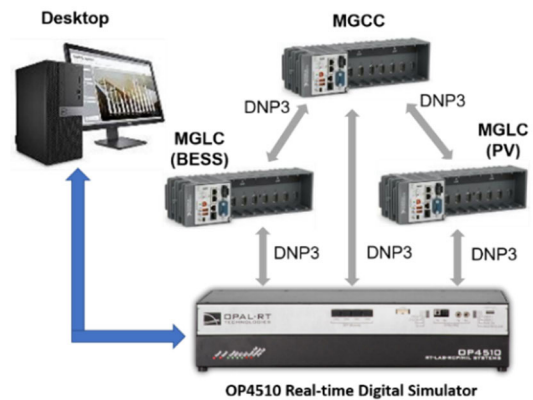

FIGURE 6. OPAL-RT HIL test setup. (Desktop PC).

The MG circuit model is based on the GridLAB-D taxonomy feeder graph R1-12.47-4 developed by PNNL [36]. It is built in MATLAB/Simulink and modified by adding one main grid interface, two BESSs, one PV array system, and one backup generator. As shown in Figure 7, the circuit is divided into eight load sections by smart switches and can be split into two sub-MGs. One sub-MG is supported by one BESS,
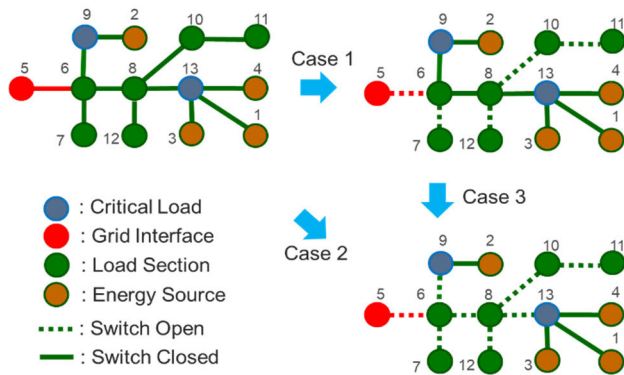
FIGURE 7. MG topology changes during planned islanding.

one solar PV installation, and one backup generator, while the other sub-MG is supported by the second BESS. Also, each sub-MG has one grounding transformer. The location of smart switches, and the sizes of BESSs, PV and backup generator are designed by using the method introduced in Section III. The capacities of the resources and grounding transformers are given in TABLE 4.

TABLE 4. Capacities of resources and grounding transformers.

	Capacity
Solar PV Installation	2 MW
BESS1	280 kW / 600 kWh
BESS2	280 kW / 600 kWh
Backup Generator	500 kW
Grounding Transformer 1	300 kVA
Grounding Transformer 2	300 kVA

2) SELECTED TEST RESULTS

As discussed in Section II, the proposed flexible MG features functions like enhanced planned islanding, islanded operation with dynamic boundary, and reconnection. Test results under these three scenarios are presented below.

a: PLANNED ISLANDING

The objective of the planned islanding is to minimize the difference in active power flow before and after the planned islanding operation. This is designed to protect the sources in the MGs. The planned islanding function utilizes the topology identification function and PQ balance to predict the BESS output power and generate switch control signals. Different from conventional MGs, the planned islanding of the flexible MG in this paper has more possible scenarios. Examples are:

- Grid-connected to the whole (one merged) MG;
- Grid-connected to two sub-MGs;
- One merged MG to two sub-MGs.

The MG topology changes during planned islanding are given in Figure 7.

These three test cases are representative for planned islanding in a multiple source MG that sees more possible islanding

routes. As shown in Figure 8, it can be observed that the active power from the BESSs for Case 1 and Case 2 have a minimal difference before and after the planned islanding, which verify the effectiveness of the planned islanding control. The active power flow difference in Case 3 is larger because the BESSs are in voltage control mode when the merged MG is islanded.
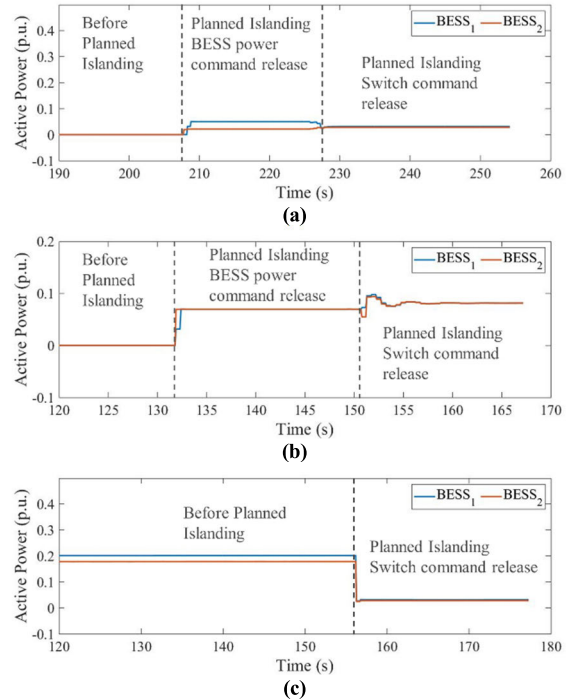

FIGURE 8. BESS active power output. (a) Case 1: Grid-connected to one merged MG; (b) Case 2: Grid-connected to two sub-MGs; (c) Case 3: One merged MG to two sub-MGs.

b: ISLANDED OPERATION WITH DYNAMIC BOUNDARY

The test case for the islanded operation covers the operation of separate sub-MGs, merging, operation of the merged MG, and PV curtailment/release. To cover these operation scenarios when islanded, the PV generation was intentionally increased to trigger the PQ balance function for boundary change or source control. The criteria for triggering PQ balance actions are BESS output hitting the discharging or charging power thresholds (caused by the PV variations). The thresholds were set to $\pm$ 200kW (or $\pm$ 0.2 p.u. on the 1 MW system base) for both BESSs in this case, and it can be reconfigured as needed in the algorithm. Figure 9 shows typical topologies of the MG during the islanded operation test.

The test started with two separate sub-MGs as in Figure 9(a), where the two sources in two different locations were operated independently. As the PV generation increased, sub-MG 1 expanded its boundary until it touched sub-MG 2 at the switch between Node 6 and Node 9, as in Figure 9(b). The PQ balance function detected the boundary
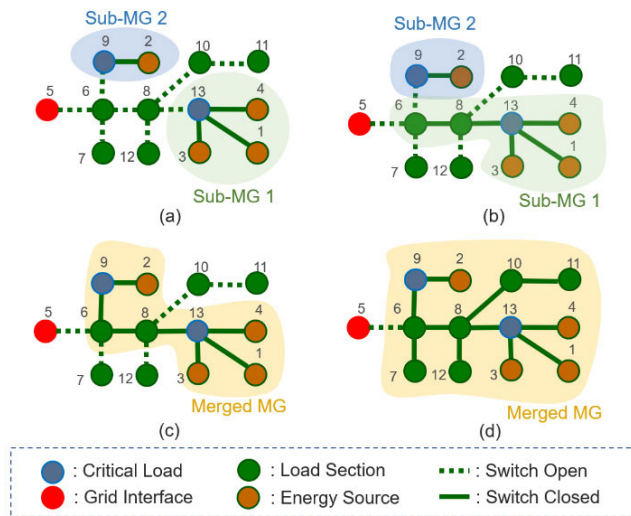
FIGURE 9. MG topology changes during islanded operation (a) Separate sub-MGs; (b) Sub-MGs before merging; (c) Merged MG; (d) Merged MG at its maximum boundary.

FIGURE 10. Power, frequency, and voltage variations during the islanded operation test on HIL.

touch and initiated merging through the reconnection function. After successfully merging, the two combined sub-MGs were operated as one merged MG, as shown in Figure 9(c). The MGCC continued to expand the boundary of the merged MG as the PV generation kept increasing until the MG reached its maximum boundary as in Figure 9(d). At this point, the MG could not further expand the boundary, but the PV generation continued to increase. As a response, the PQ balance function initiated PV curtailment to bring the BESS power close to zero. The reason why the PV curtailment is designed to bring the BESS output to zero, instead of maximum allowable BESS power, is that PV curtailment often happens when the solar generation ramps up rather quickly and thus, the BESS should have enough safety margin under such extreme conditions. The PQ Balance, being a short-term balancing module, prioritizes the safe operation of the equipment and prevents BESS and other resources from tripping themselves under extreme conditions. Under normal operations, though, the PQ Balance will take recommendations from the Energy Management module to facilitate long-term goals if possible, including the BESS state of charge (SOC). The curtailment was released when the PV generation decreased to a safer level that does not lead to BESS power threshold violations.

Figure 10 shows the PV generation, the power output of BESSs and backup generator, and frequency/voltage at the source locations during the test. The green dash lines divide the process into four stages as marked with circled numbers in green. The red dash lines are time instances when boundary changes happened.

Stage one is the operation of multiple sub-MGs, where the sub-MG 1 expanded its boundary due to the increasing PV generation, until it touches the boundary of sub-MG 2, corresponding to Figure 9(b). The switch between Node 13 and
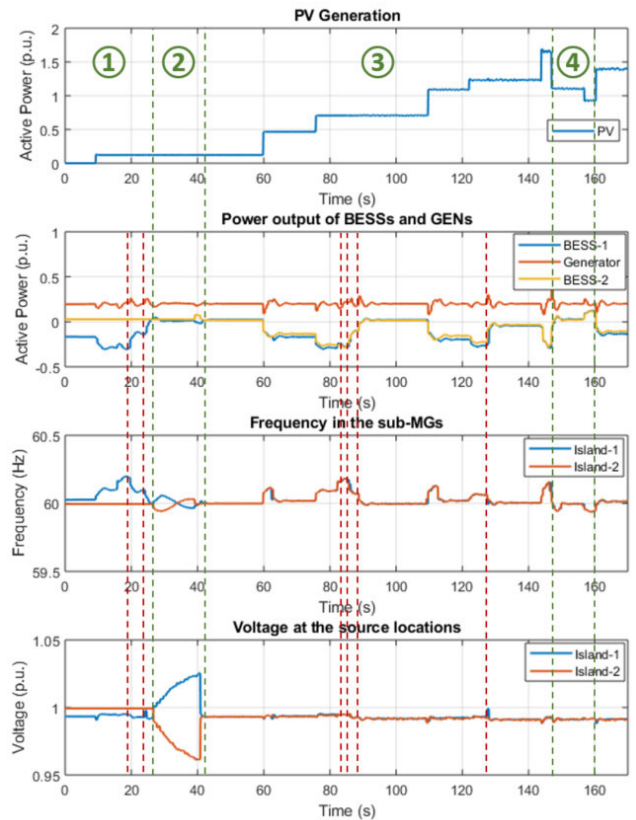
Node 8 and the switch between Node 8 and Node 6 were closed at t = 19 s and t = 24 s, as indicated by the two red dash lines in stage one.

Stage two is the merging of the two sub-MGs. The PQ balance function initiated the merging, and the reconnection function synchronizes the two sub-MGs by adjusting the sources to have their voltage magnitude and angle match each other. The switch between Node 6 and Node 9 was closed when synchronization was achieved.

In stage three, the merged MG expanded its boundary due to the increasing PV generation. Four load sections were picked up consecutively in this process, LS7, LS12, LS10, and LS11, as indicated by the four red dash lines in stage three. At the beginning of stage four, the merged MG has already reached its maximum boundary and the PV generation provided more power into the BESSs that exceeded their safety margin. The PQ balance function issued a PV curtailment command at t = 146 s and brought the power flow into the BESSs close to 0 W. At t = 160 s, the PV curtailment was released since the PV generation decreased to a safe level for the BESSs.

The maximum frequency deviation during a transient (except during the merging process when the source frequency and voltage were intentionally manipulated for synchronization) was 0.2 Hz, and the steady-state frequency

was always brought back to 60 Hz. The maximum voltage deviation was less than 0.01 p.u. throughout the test.

c: RECONNECTION

As mentioned in Section II, the two sub-MGs can be reconnected to the main grid individually, or they can be merged as one MG and then reconnected to the main grid at once. Therefore, there are two test cases for reconnection. The former one is similar to the reconnection function of conventional MGs. The latter is illustrated below.

Figure 11 shows the MG topology changes during reconnection. The two sub-MGs are merged into one islanded MG by closing the switch between Node 6 and Node 9, and then reconnected to the main grid by closing the switch between Node 5 and Node 6. Figure 12 shows the output power, frequency of the sources, and angle differences between the switches being closed in the process. After reconnecting to the main grid, the output power from the BESSs reduces to 0 W, according to the commands from the system operator.
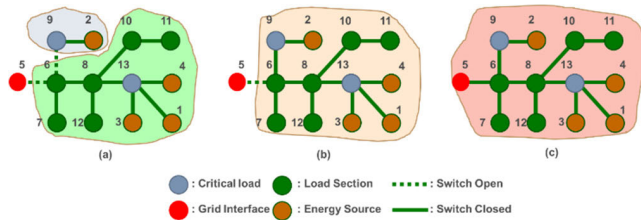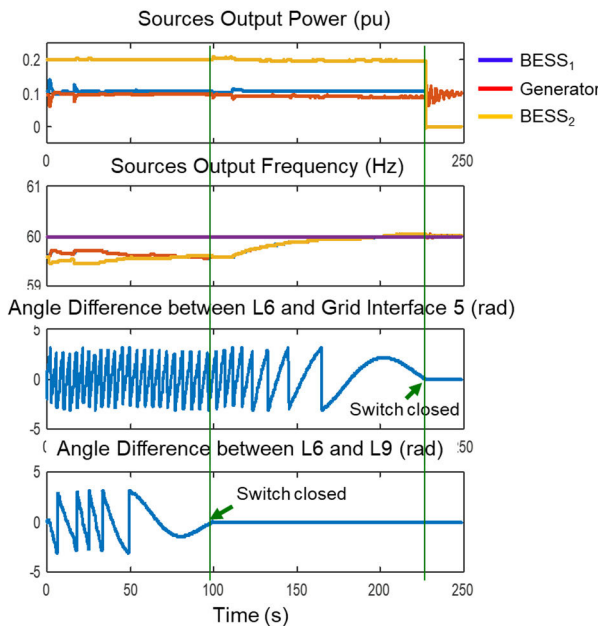

FIGURE 11. MG topology changes during reconnection.

FIGURE 12. Active power, frequency, and angle difference when reconnecting to the main grid.

B. HIL TEST ON CONVERTER-BASED HTB
1) HTB-BASED TEST SETUP

The HTB at UTK is a reconfigurable converter-based power grid emulation platform [37]. In the HTB, power converters are utilized to emulate MG components, including grid

interfaces, loads, and DERs. Compared with the OPAL-RT simulator, HTB has real power flow in the setup and can emulate more practical grid and control factors that are critical but may not be included in most simulations. The practical factors include communication delays, measurement noise or error, hardware protection, and switching actions of power converter switches. By conducting HTB testing, the MG controller can be further evaluated and better prepared for field deployment.

In the HTB testing, the MG designed in Section III is scaled from 12.47 kV, 1 MW to 100 V, 1.732 kW, containing two potential sub-MGs. The HTB-based HIL test setup is given in Figure 13. The HTB emulates the DMS/SCADA system, MG topology, smart switches, grid interfaces, loads, DERs, etc. to form a converter-based MG. The developed MGCC as well as local DER MGLCs are placed in-the-loop for testing.
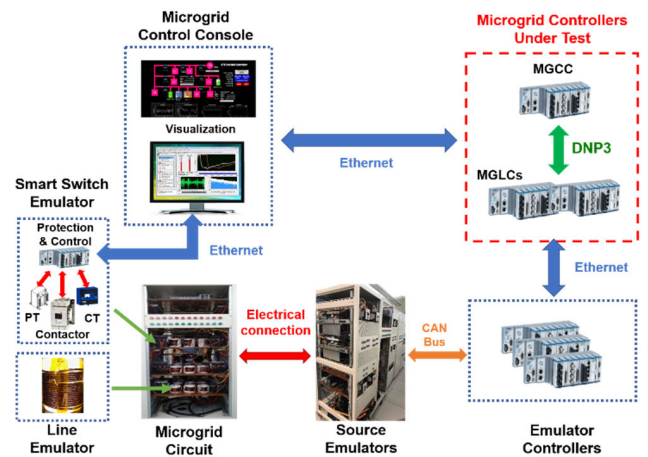

FIGURE 13. HTB-based HIL test setup.

2) SELECTED TEST RESULTS

The test case on HTB for islanded operation is similar to that of HIL testing using the digital simulator. Figure 14 shows the topology changes happened during the islanded operation test, and Figure 15 shows the variations in power, frequency, and voltage during the testing.

The test started with two sub-MGs with minimum boundary, as in Figure 14(a). With the increasing PV generation, the boundary of sub-MG 1 expanded until it touches that of sub-MG 2, as shown in Figure 14(b) and stage one in Figure 15. Five load sections, LS4, LS5, LS3, LS7, LS2, were picked up consecutively as indicated by the five red dash lines in stage one. Stage two in Figure 15 shows the merging process that combines the two sub-MGs, and stage three shows the PV curtailment (t = 124 s) and release (t = 136 s). Since the HTB has actual current, voltage, and power running on the testbed, oscilloscope probes were hooked up to the equipment to record the waveforms during the test. Figure 16 shows a representative part of the recording where LS5, LS3, LS7, and LS2 were picked up during the boundary expansion.
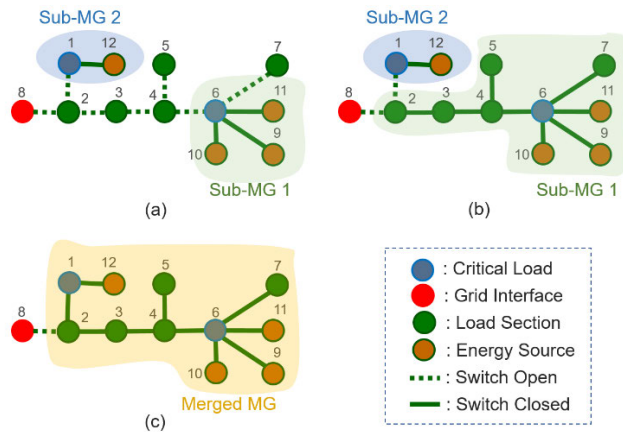
FIGURE 14. MG topology changes during the islanded operation. (a) Separate sub-MGs; (b) Sub-MGs before merging; (c) Merged MG at its maximum boundary.
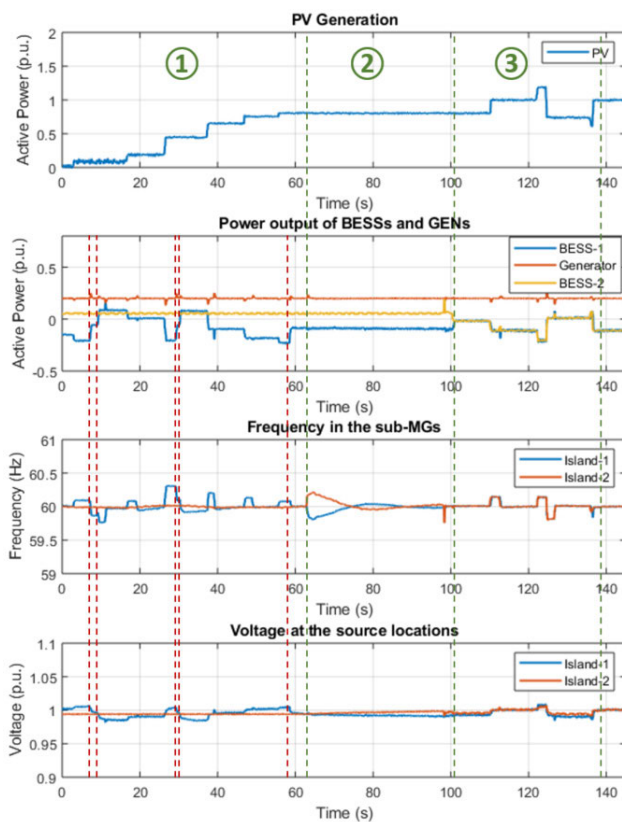

FIGURE 15. Power, frequency, and voltage variations during the islanded operation test on HTB.

The maximum frequency deviation during a transient was 0.3 Hz, and the steady-state frequency always stabilized at 60 Hz. The maximum voltage deviation was less than 0.01 p.u. throughout the test.

The dynamic boundary for both separate sub-MGs and merged MG and the merging process benefit from the capability of the controller to automatically recognize and adapt to arbitrary topologies, which enables the controller to easily

migrate from one testbed/topology to another with minimum effort and cost. Compared to the OPAL-RT simulator testing, the controller HTB testing considers more practical factors such as measurement noise/error, communication delays, mechanical switching actions, etc., which makes the controller more robust, practical, and ready for field deployment.

VI. FIELD DEPLOYMENT AT MUNICIPAL UTILITY

A smart and flexible MG was deployed at the municipal utility Electrical Power Board (EPB) in Chattanooga, Tennessee. This section introduces its components, control and communication structure, its basic operation modes, and a few selected field test results.

A. FIELD DEPLOYMENT OF MG AND MGCC

Figure 17 shows the diagram of the MG deployed at EPB. This MG consists of solar PV installation, two 280 kW/255 kWh BESSs, one 300 kVA grounding transformer, one 423 kW backup generator, and several load sections (LS1 to LS6) divided by smart switches.

Additionally, there is one 300 kVar fixed capacitor bank in LS3, and one 300 kVar switchable capacitor bank in LS4. S0101, S0102, S0103, S0104, S0105, and S0106 are normally-closed smart switches (in red), while S0201, S0301, S0302, S0401, S0502 are normally-open smart switches (in green). The load section LS5 is the critical load.

The MG control and communication system is also illustrated in Figure 17. This MG employs a hierarchical control structure: central control level and device control level. At the central control level, one MGCC is deployed to perform monitoring and control of the entire MG. At the device control level, smart switches, BESS inverters, backup generator and solar PV inverters have their own built-in control functions.

The communication is based on DNP3. However, a real-time automation controller (RTAC) is installed as the protocol converter (Modbus to DNP3) to facilitate the communication between the BESSs and both the MGCC and DMS/SCADA. Similarly, another RTAC is used as the protocol converter between the backup generator and MGCC (or DMS/SCADA). Additionally, an analog signal can be sent by the RTAC (or an SEL relay) to BESSs (or the generator) to switch their operation mode between grid-forming and grid-following. This MG features multiple grid interfaces and dynamic boundaries. The MG is normally connected to Feeder #1 to operate in grid-connected mode. The BESSs and the backup generator can be started for demand reduction if needed. When Feeder #1 is not available, the MG could be connected to one of the adjacent feeders, e.g., Feeder #2. If none of the five feeders are available due to extreme weather or power outage events, the MG can operate in the islanded mode, in which the MG could expand or shrink its boundary by picking up or shedding load sections based on available power generated inside the MG. For instance, if there is adequate power in the MG, load sections LS4, LS3, and LS2 can also be served in addition to the critical load section LS5. If there is not adequate power
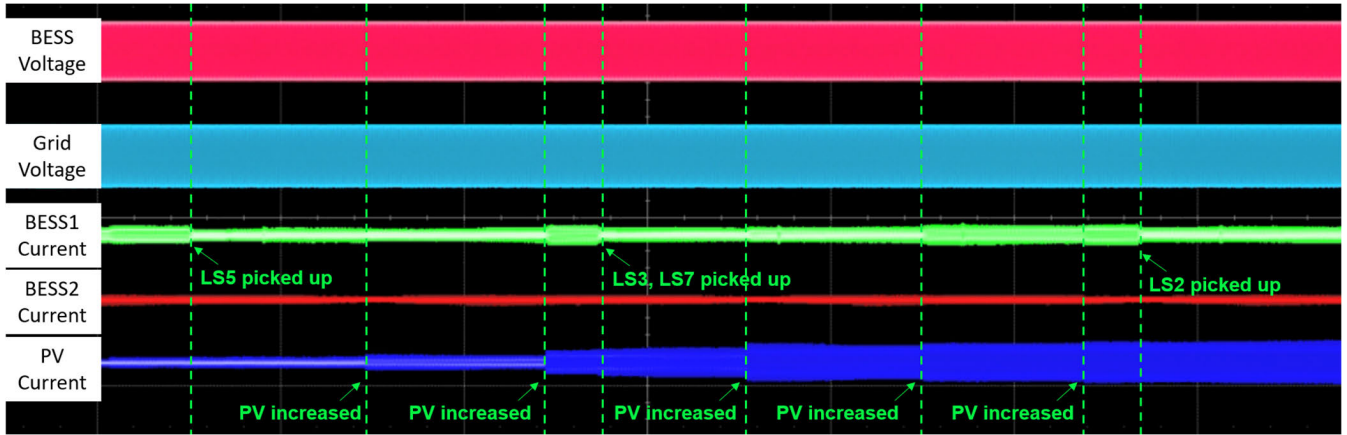
FIGURE 16. Oscilloscope waveform recording of the boundary expansion (LS5, LS3, LS7, LS2 picked up).
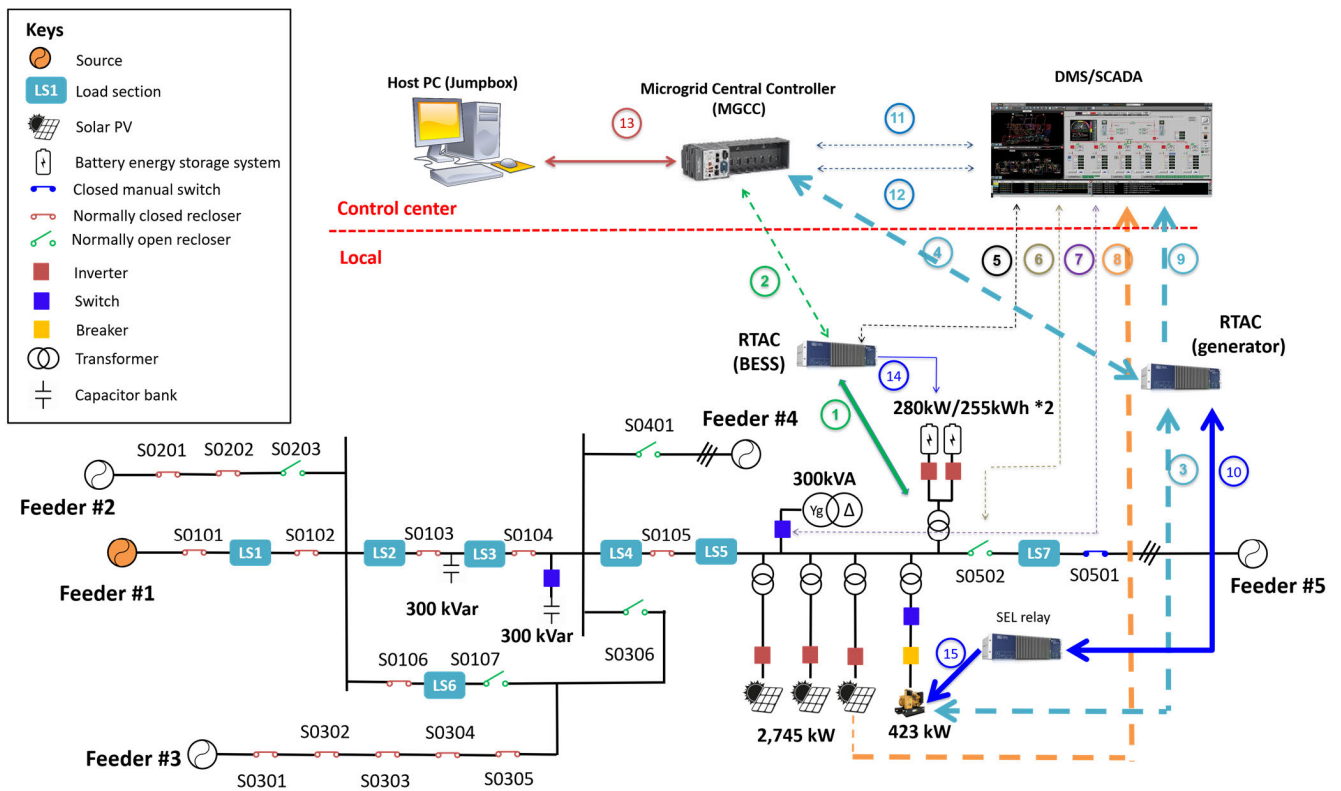

FIGURE 17. MG and MG controller deployed at a municipal utility.

from PVs and BESSs, switches S0103, S0104, and S0105 might be opened to ensure the safe operation of the critical load section LS5. Compared with conventional MGs with fixed boundaries, this MG could have different PCCs when reconnecting to Feeder #1. The PCC could be S0102, S0103, S0104, or S0105, depending on the available power inside the MG. Moreover, the MG can be reconnected to other adjacent feeders through S0201, S0301, S0302, S0401, or S0501 as the PCC, allowing a more flexible operation. When any of the feeders becomes available, the MG will reconnect to that feeder and operate in the grid-connected mode again.

B. SELECTED FIELD TEST RESULTS

During the field tests, the maximum MG boundary was limited to S0104 (Figure 17) to not interrupt too many load sections, although the MG boundary can be extended to S0101 if needed. Also, during the field tests, the manual switch S0501 on Feeder #5 was opened so that the load section LS7 could be served by the MG resources. Multiple scenarios were tested, including grid-connected mode operation, islanded operation (boundary shrinking and boundary expanding), and transitions (black start and reconnection).
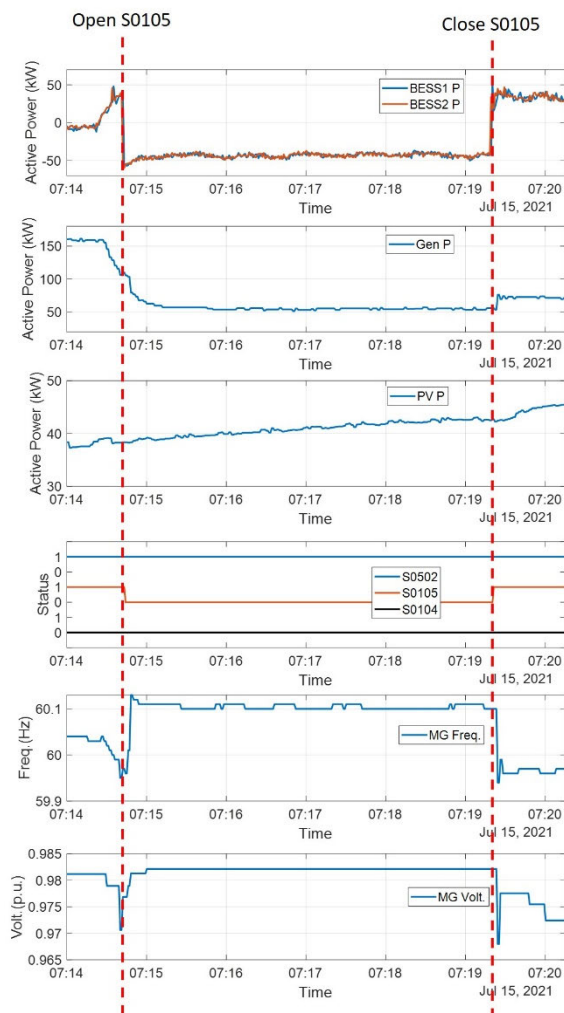
FIGURE 18. Field test result: MG boundary shrinking and expanding.

Figure 18 shows the field test results of boundary shrinking and boundary expanding. Prior to the boundary shrinking, the MG was operating in the islanded mode, and LS4, LS5, and LS7 were served by the MG. At 07:14:29, the generator active power output was reduced intentionally to mimic a "low generation" scenario to trigger the boundary shrinking. At 07:14:44, S0105 was opened by the MGCC to shed LS4 and shrink the MG boundary to S0105. Two BESSs switched their operation mode from discharging to charging due to the extra generation within the MG after the boundary shrinking. Also, the MG frequency increased to 60.13 Hz, while the MG voltage dropped to 0.971 p.u. and then returned to 0.982 p.u.

With the PV output power kept increasing, the MGCC expanded the MG boundary by closing S0105 to pick up LS4 at 07:19:23. After the MG boundary expanded, two BESSs switched their operation mode from charging to discharging. Also, the MG frequency dropped to 59.95 Hz, while the MG voltage dropped to 0.968 p.u. after the MG boundary expanded. The test results demonstrated that the developed MGCC can flexibly expand or shrink the MG boundary

according to the available power generation in the islanded MG. It is noted that the dynamic boundary control can take various measures to maintain the active power and reactive power balance in the islanded MG, e.g., BESS operation mode switching (charging or discharging), solar PV curtailment, and smart switch operation to pick up or shed load sections. This differs from conventional load shedding schemes. More field test results will be reported by the authors in a separate paper.

VII. SUMMARY
The increasing deployment of smart switches facilitates the implementation of flexible MGs with dynamic boundaries. The main advantages and differences of flexible MGs, as compared to conventional MGs with fixed boundaries, are discussed in detail. The main challenges in flexible MG design are identified and addressed. Moreover, a controller is designed and implemented to enable the operation of such a flexible MG with dynamic boundaries. The open-source controller based on LabVIEW is accessible on GitHub [38]. The controller has been fully validated on an OPAL-RT-based HIL test setup and a reconfigurable convert-based HTB. A realistic flexible MG and its controller have been deployed at a municipal utility.

REFERENCES
[1] U.S. Department of Energy. *The Role of Microgrids in Helping to Advance the Nation's Energy System.* Accessed: Dec. 3, 2021. [Online]. Available: https://www.energy.gov/oe/activities/technology-development/grid-modernization-and-smart-grid/role-microgrids-helping

[2] D. T. Ton and M. A. Smith, "The U.S. Department of energy's microgrid initiative," *Electr. J.*, vol. 25, no. 8, pp. 84–94, Oct. 2012.

[3] M. E. Nassar and M. M. A. Salama, "Adaptive self-adequate microgrids using dynamic boundaries," *IEEE Trans. Smart Grid*, vol. 7, no. 1, pp. 105–113, Jan. 2016.

[4] Y.-J. Kim, J. Wang, and X. Lu, "A framework for load service restoration using dynamic change in boundaries of advanced microgrids with synchronous-machine DGs," *IEEE Trans. Smart Grid*, vol. 9, no. 4, pp. 3676–3690, Jul. 2018.

[5] F. Wang, X. Shi, L. M. Tolbert, Y. Ma, Y. Liu, and L. Zhu, "Microgrids with dynamically configurable boundaries including multiple main grid feeder coupling locations and methods of operating the same," U.S. Patent 10 447 038 B2. Oct. 15, 2019. [Online]. Available: https://patents.google.com/patent/US10447038B2/en?q=Microgrids+dynamically+configurable+boundaries+including+multiple+main+grid+feeder+coupling+locations+and+methods+of+operating+the+same&oq=Microgrids+with+dynamically+configurable+boundaries+including+multiple+main+grid+feeder+coupling+locations+and+methods+of+operating+the+same

[6] J. Shi, A. Maitra, and B. Rogers, "A smart and flexible microgrid with dynamic boundary and intelligent open-source controller," Electr. Power Res. Inst., White Paper 3002014310, Sep. 2018. [Online]. Available: https://www.epri.com/research/products/000000003002014310

[7] *Microgrids—Part 1: Guidelines for Microgrid Projects Planning and Specification*, Standard IEC TS 62898-1, May 2017.

[8] *HOMER Energy*. Accessed: Dec. 3, 2021. [Online]. Available: https://www.homerenergy.com/products/pro-vs-grid.html

[9] M. Stadler, G. Cardorso, S. Mashayekh, and N. DeForest, "Distributed energy resources customer adoption model plus (DER-CAM+), version 1.0.0," Lawrence Berkeley Nat. Lab., Berkeley, CA, USA, Tech. Rep. DER-CAM+; 004669MLTPL00, Mar. 2016.

[10] J. Eddy, N. E. Miner, and J. Stamp, "Sandia's microgrid design toolkit," *Electr. J.*, vol. 30, no. 4, pp. 62–67, May 2017.

[11] R. P. Jensen, J. E. Stamp, J. P. Eddy, J. M. Henry, K. Munoz-Ramos, and T. Abdallah, "Methodology for preliminary design of electrical microgrids," Sandia Nat. Laboratories (SNL-NM), Albuquerque, NM, USA, Tech. Rep. SAND2015–8433, Sep. 2015.

[12] *IEEE Standard for the Specification of Microgrid Controllers Management System*, Standard 2030.7-2018, IEEE, 2017.

[13] A. Kowalczyk, A. Włodarczyk, and J. Tarnawski, "Microgrid energy methods and models in automation and robotics (MMAR)," in *Proc. 21st Int. Conf.*, Miedzyzdroje, Poland, Aug. 2016, pp. 157–162.

[14] S. Bracco, F. Delfino, F. Pampararo, M. Robba, and M. Rossi, "A dynamic optimization-based architecture for polygeneration microgrids with tri-generation, renewables, storage systems and electrical vehicles," *Energy Convers. Manage.*, vol. 96, pp. 511–520, May 2015.

[15] GE. *Grid IQ Microgrid Control System*. Accessed: Dec. 3, 2021. [Online]. Available: https://www.gegridsolutions.com/multilin/catalog/mcs.htm

[16] Eaton. *Eaton's Intelligent Grid Solutions—Microgrid and Energy Storage Systems*. Accessed: Dec. 3, 2021. [Online]. Available: https://www.ncsl.org/Portals/1/Documents/energy/Paolettipresent.pdf

[17] Spirae. *Microgrid Solution*. Accessed: Dec. 3, 2021. [Online]. Available: http://www.spirae.com/microgrid/about-microgrid

[18] S. Kavitha, R. Jayashree, I. M. Rafeequdin, and K. Danasagaran, "Defining the boundaries of microgrids in a large distribution system ensuring supply security," in *Proc. 7th Int. Conf. Power Syst. (ICPS)*, Pune, India, Dec. 2017, pp. 277–282.

[19] C. Chen, J. Wang, F. Qiu, and D. Zhao, "Resilient distribution system by microgrids formation after natural disasters," *IEEE Trans. Smart Grid*, vol. 7, no. 2, pp. 958–966, Mar. 2016.

[20] T. Zhao, J. Wang, and X. Lu, "An MPC-aided resilient operation of multi-microgrids with dynamic boundaries," *IEEE Trans. Smart Grid*, vol. 12, no. 3, pp. 2125–2135, May 2021.

[21] Y. Du, X. Lu, J. Wang, and S. Lukic, "Distributed secondary control strategy for microgrid operation with dynamic boundaries," *IEEE Trans. Smart Grid*, vol. 10, no. 5, pp. 5269–5282, Nov. 2018.

[22] T. Zhao, B. Chen, S. Zhao, J. Wang, and X. Lu, "A flexible operation of distributed generation in distribution networks with dynamic boundaries," *IEEE Trans. Power Syst.*, vol. 35, no. 5, pp. 4127–4130, Sep. 2020.

[23] *IEEE Standard for the Testing of Microgrid Controllers*, Standard 2030.8, IEEE, 2018.

[24] X. Hu, T. Liu, C. He, Y. Ma, Y. Su, H. Yin, F. Wang, L. M. Tolbert, S. Wang, and Y. Liu, "Real-time power management technique for microgrid with flexible boundaries," *IET Gener., Transmiss. Distrib.*, vol. 14, no. 16, pp. 3161–3170, Aug. 2020.

[25] H. Yin, Y. Ma, L. Zhu, X. Hu, Y. Su, J. Glass, F. Wang, Y. Liu, and L. M. Tolbert, "Hierarchical control system for a flexible microgrid with dynamic boundary: Design, implementation and testing," *IET Smart Grid*, vol. 2, no. 4, pp. 669–676, Sep. 2019.

[26] X. Hu, T. Liu, Y. Ma, Y. Su, H. Yin, L. Zhu, F. Wang, L. M. Tolbert, and Y. Liu, "Two-stage EMS for distribution network under defensive islanding," *IET Gener., Transmiss. Distrib.*, vol. 13, no. 18, pp. 4073–4080, Sep. 2019.

[27] Y. Ma, X. Hu, H. Yin, L. Zhu, Y. Su, F. Wang, L. M. Tolbert, and Y. Liu, "Real-time control and operation for a flexible microgrid with dynamic boundary," in *Proc. IEEE Energy Convers. Congr. Expo. (ECCE)*, Portland, OR, USA, Sep. 2018, pp. 5158–5163.

[28] D. Li, Y. Ma, C. Zhang, H. Yin, I. Ray, Y. Su, L. Zhu, F. Wang, and L. M. Tolbert, "Development of a converter based microgrid test platform," in *Proc. IEEE Energy Convers. Congr. Expo. (ECCE)*, Baltimore, MD, USA, Sep. 2019, pp. 6294–6300.

[29] S. Zhen, Y. Ma, F. Wang, and L. M. Tolbert, "Operation of a flexible dynamic boundary microgrid with multiple islands," in *Proc. IEEE Appl. Power Electron. Conf. Expo. (APEC)*, Anaheim, CA USA, Mar. 2019, pp. 548–554.

[30] J. Dong, L. Zhu, Y. Su, Y. Ma, Y. Liu, F. Wang, L. M. Tolbert, J. Glass, and L. Bruce, "Battery and backup generator sizing for a resilient microgrid under stochastic extreme events," *IET Gener., Transmiss. Distribution*, vol. 12, no. 20, pp. 4443–4450, Nov. 2018.

[31] *Effective Grounding and Inverter-Based Generation: A 'New' Look at an 'Old' Subject*. EPRI Report. Accessed: Dec. 3, 2021. [Online]. Available: https://files.engineering.com/download.aspx?folder=4b81017c-9b50-486d-9c9c-adfa5f1c9260&file=EPRI_Parallel_DG.pdf

[32] *IEEE Recommended Practice for Electric Power Distribution for Industrial Plants*, Standard 141-1993, IEEE, Apr. 1994, pp. 1–768.

[33] *IEEE Guide for the Application of Neutral Grounding in Electrical Utility Systems–Part I: Introduction*, Standard C62.92.1-2016 IEEE, Mar. 2017, pp. 1–38.

[34] *IEEE Standard for Requirements, Terminology, and Test Procedures for Neutral Grounding Devices*, Standard C57.32-2015 IEEE, 2016.

[35] L. Zhu, I. Ray, F. Wang, L. M. Tolbert, Y. Liu, Y. Ma, H. Yin, and D. Li, "Methods, systems, and computer readable media for protecting and controlling a microgrid with a dynamic boundary," U.S. Patent 16 775 836, Nov. 5, 2020. [Online]. Available: https://patents.google.com/patent/US20200350761A1/en

[36] BetterGrid.org. (Nov. 2008). *PNNL Taxonomy Feeders—Region 1—Feeder 4*. [Online]. Available: https://sourceforge.net/p/gridlab-d/code/HEAD/tree/Taxonomy_Feeders/R1-12.47-4.glm

[37] L. M. Tolbert, F. Wang, K. Tomsovic, K. Sun, J. Wang, Y. Ma, and Y. Liu, "Reconfigurable real-time power grid emulator for systems with high penetration of renewables," *IEEE Open Access J. Power Energy*, vol. 7, pp. 489–500, 2020.

[38] *DynaMic_Basic and DynaMic_NET_MG_Basic*. Accessed: Dec. 3, 2021. [Online]. Available: https://github.com/GeniusMicrogrid/DynaMic_Basic
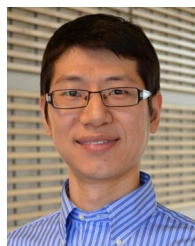
LIN ZHU (Senior Member, IEEE) received the B.S. and Ph.D. degrees in electrical engineering from the Huazhong University of Science and Technology, in 2005 and 2011, respectively.

He was a Research Assistant Professor with the Min H. Kao Department of Electrical Engineering and Computer Science, The University of Tennessee, Knoxville (UTK). Earlier, he worked as a Research Associate and a Postdoctoral Researcher at UTK. In August 2021, he joined Electric Power Research Institute as the Technical Leader of transmission operations and planning. His current research interests include power system dynamics, renewable energy integration, smart distribution grid, and microgrid.

CHENGWEN ZHANG (Graduate Student Member, IEEE) received the B.S. and M.S. degrees in electrical engineering from the Huazhong University of Science and Technology, China, in 2015 and 2018, respectively. He is currently pursuing the Ph.D. degree with the Department of Electrical Engineering and Computer Science, The University of Tennessee, Knoxville. His research interests include microgrid operation and control, large-scale power system dynamics, data analysis, and protection.

HE YIN (Member, IEEE) received the B.S. and Ph.D. degrees in electrical and computer engineering from the University of Michigan-Shanghai Jiao Tong University Joint Institute, Shanghai Jiao Tong University, Shanghai, China, in 2012 and 2017, respectively.

He is currently a Postdoctoral Researcher at the Center for Ultra-Wide-Area Resilient Electric Energy Transmission Networks (CURENT), The University of Tennessee, Knoxville, TN, USA. His research interests include optimization and decentralized control of microgrid and PMU design.

DINGRUI LI (Student Member, IEEE) received the B.S. degree from the Department of Electrical Engineering, Tsinghua University, Beijing, China, in 2017. He is currently pursuing the Ph.D. degree in power electronics with The University of Tennessee, Knoxville, TN, USA.

His research interests include power converter in grid applications, medium voltage multilevel converters, converter paralleling, and microgrids.
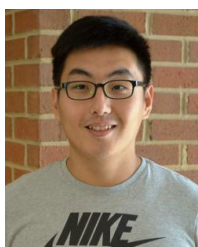
YU SU (Graduate Student Member, IEEE) received the B.Eng. degree from Tsinghua University, Beijing, China, in 2015. He is currently pursuing the Ph.D. degree with The University of Tennessee, Knoxville, TN, USA. His research interests include microgrid design and control optimization, renewable integration in electrical power systems, and applications of machine learning methods in power systems.

ISHITA RAY (Member, IEEE) received the B.E. degree in electrical engineering from Panjab University, in 2013, the M.S. degree in electrical and computer engineering from the Georgia Institute of Technology, Atlanta, in 2014, and the Ph.D. degree in energy science and engineering from The University of Tennessee, Knoxville, in 2021. She worked on various projects related to microgrids with the CURENT ERC and the Oak Ridge National Laboratory. She is currently working as a Senior Modeling Engineer at TAE Technologies Inc. Her research interests include renewable energy systems, power system and inverter modeling, microgrid operation and control, and energy economics and policy.

JIAOJIAO DONG (Senior Member, IEEE) received the B.S. degree in information engineering and the M.S. and Ph.D. degrees in automation control from Xi'an Jiaotong University, China, in 2008, 2011, and 2016, respectively. She is currently a Postdoctoral Researcher at The University of Tennessee, Knoxville, USA. Her research interests include power system planning and operation, renewable energy integration, and microgrids.

FRED WANG (Fellow, IEEE) received the B.S. degree in electrical engineering from Xi'an Jiaotong University, Xi'an, China, in 1982, and the M.S. and Ph.D. degrees in electrical engineering from the University of Southern California, Los Angeles, CA, USA, in 1985 and 1990, respectively.

He was a Research Scientist with the Electric Power Laboratory, University of Southern California, from 1990 to 1992. He joined the GE Power Systems Engineering Department, Schenectady, NY, USA, in 1992, as an Application Engineer. From 1994 to 2000, he was a Senior Product Development Engineer with GE Industrial Systems, Salem, VA, USA. From 2000 to 2001, he was the Manager of the Electronic and Photonic Systems Technology Laboratory, GE Global Research Center, Schenectady, NY, USA, and Shanghai, China. In 2001, he joined the Center for Power Electronics Systems (CPES), Virginia Tech, Blacksburg, VA, USA, as a Research Associate Professor, and became an Associate Professor, in 2004. From 2003 to 2009, he also served as the CPES Technical Director. Since 2009, he has been with The University of Tennessee, Knoxville, TN, USA, and the Oak Ridge National Laboratory, as a Professor, and the Condra Chair of Excellence in power electronics. He is currently a Founding Member and the Technical Director of the Multi-University NSF/DOE Engineering Research Center for Ultra-wide-area Resilient Electric Energy Transmission Networks (CURENT) led by The University of Tennessee. His research interests include power electronics and power systems. He is a fellow of the U.S. National Academy of Inventors.

LEON M. TOLBERT (Fellow, IEEE) received the bachelor's, M.S., and Ph.D. degrees in electrical engineering from the Georgia Institute of Technology, Atlanta, in 1989, 1991, and 1999, respectively.

He is currently a Chancellor's Professor and the Min H. Kao Professor with the Department of Electrical Engineering and Computer Science, The University of Tennessee. He is a Founding Member and a Testbed Thrust Leader for the NSF/DOE Engineering Research Center, Center for Ultra-Wide-Area Resilient Electric Energy Transmission Networks (CURENT). He is also an Adjunct Participant with the Oak Ridge National Laboratory. His research interests include the utility applications of power electronics, microgrids, electric vehicles, and wide bandgap semiconductors.

Dr. Tolbert was a recipient of the 2001 IEEE Industry Applications Society Outstanding Young Member Award and Eight Prize Paper Awards from the IEEE Industry Applications Society and the IEEE Power Electronics Society. He was the Paper Review Chair for the Industry Power Converter Committee of the IEEE Industry Applications Society, from 2014 to 2017. He was an Associate Editor of the IEEE Transactions on Power Electronics, from 2007 to 2013. He is the Academic Deputy Editor-in-Chief of *IEEE Power Electronics Magazine* (2021–2023).

YILU LIU (Fellow, IEEE) received the B.S. degree from Xi'an Jiaotong University, China, and the M.S. and Ph.D. degrees from The Ohio State University, Columbus, in 1986 and 1989, respectively. She was a Professor with Virginia Tech, where she led the effort to create the North American power grid frequency monitoring network, which is currently operated with The University of Tennessee (UTK), Knoxville, and the Oak Ridge National Laboratory (ORNL) as GridEye. She is a Governor's Chair with UTK and ORNL. She is also the Deputy Director of the DOE/NSF—co-funded engineering research center, Center for Ultra-Wide-Area Resilient Electric Energy Transmission Networks (CURENT). Her current research interests include power system wide-area monitoring and control, large interconnection-level dynamic simulations, electromagnetic transient analysis, and power transformer modeling and diagnosis. She is a member of the U.S. National Academy of Engineering and the National Academy of Inventors.

YIWEI MA (Member, IEEE) received the B.S. and M.S. degrees in electrical engineering from Tsinghua University, Beijing, China, in 2009 and 2011, respectively, and the Ph.D. degree in electrical engineering from The University of Tennessee, Knoxville, TN, USA, in 2019. He is currently a Research Engineer with Electric Power Research Institute, Knoxville. His research interests include modeling and control of power electronics interfacing converters for renewable energy sources, multilevel converters, and microgrids.

SAMUEL DELAY received the B.S. degree in electrical engineering from The University of Tennessee, Knoxville, TN, USA, and the Master of Business Administration degree from The University of Tennessee at Chattanooga, TN, USA. He is currently a Senior Program Manager at TVA Strategic Research-Technology Innovation. His research interests include customer technology, new business and grid services–operations research and support, and technology innovation.

PETER GREGORY is currently the Founder of Green Energy Corporation and serves as the Chief Executive Officer and the Chairperson for the Board. For over 25 years, he has developed his skill set and management capacity in industry operations and has served as a CEO, a CFO, and a VP of engineering for software manufacturing companies. He founded Green Energy Corporation and held senior management positions in several companies in the utility industry.

BRUCE ROGERS received the Bachelor of Science degree (Hons.) in mechanical engineering from The University of Tennessee at Chattanooga. He is currently a Technical Executive at Electric Power Research Institute (EPRI). He has over 40 years of electric utility industry experience spanning generation, transmission, distribution, and innovation. He is responsible for development and management of major project initiatives that address the increasingly complex planning, design, construction, operation, and maintenance of a modern distribution system. He also worked with many distribution utilities to develop company-specific strategic roadmaps for modernizing their grid to meet a company's unique needs. Prior to joining EPRI, he worked over 35 years in various roles at the Tennessee Valley Authority (TVA). He was most recently responsible for managing TVA's strategic research and development activities as the Director of technology innovation. He has authored or coauthored numerous technical papers and articles within his area.

MARIO GARCIA-SANZ currently serves as a Program Director for DOE/ARPA-E. He is a University Professor at Case Western Reserve University and a Veteran of the European wind energy industry with experience designing commercial multi-megawatt wind turbines. He is also a Control Engineer, an Entrepreneur, and a Technical Leader with over 30 years of experience designing multidisciplinary systems and advanced control co-design solutions for energy companies and space agencies. He has excelled in academia and industry. He is holding appointments at the NASA Jet Propulsion Laboratory, the European Space Agency, NATO, Case Western Reserve University, Oxford University, Manchester University, the Public University of Navarra, and TECNUN. At ARPA-E, he developed the ATLANTIS Program on floating offshore wind, the SHARKS Program on tidal and riverine energy, and led the efforts on grid technology with the NODES Program, with over 40 research projects in about 30 states with a very strong multi-institution cross-collaboration.

JIM GLASS received the B.S. degree in industrial engineering from The University of Tennessee. He is currently a Senior Manager of smart grid development at EPB, Chattanooga, TN, USA. His current responsibilities include distribution automation, SCADA and distribution management systems, and demand management technology and distributed energy resources. He is also responsible for EPB's system planning and protection and controls engineering functions. Prior to joining EPB, he worked at Florida Power & Light Company for over 20 years, where he held various positions related to smart grid technology, control center management, and emergency preparedness. He is a member of The University of Tennessee at Chattanooga's (UTC) Electrical Engineering Advisory Board and an Adjunct Instructor at UTC.

MIRJANA MARDEN received the B.Sc. degree in electrical engineering from the University of Novi Sad, Serbia, in 2000, the M.Sc. degree in control systems and signal processing from Northeastern University, Boston, in 2002, and the Ph.D. degree in power systems from the Swiss Federal Institute of Technology (ETH Zurich), in 2007. She is currently serving as a Science, Engineering and Technology Advisor for the United States Department of Energy, Advanced Research Projects Agency-Energy (ARPA-E), where she is providing technical support for power system grid related programs that facilitate the integration of renewable energy, distributed power generation on the grid, and microgrids. She is leading project teams across national laboratories, academia, and industry by providing services in technical project management and federal funding acquisition. Her research interests include developing advanced control techniques to inverter-based distributed energy resources (DER) in power system microgrids, artificial intelligence applied to power systems, power system dynamics, system components, and subsystem faults.

LILIAN BRUCE received the B.S. degree in architecture from Syracuse University and the M.B.A. degree from UT Chattanooga. She is currently serving as the EPB's Senior Director for strategic planning. She is instrumental in securing over $150 million dollars in government funding for next generation technologies and research and facilitating U.S. National Labs and Community relationships. Her experience is grounded in architecture, the natural gas/power, and communications industry.

• • •